Physica B 454 (2014) 50–55

Contents lists available at ScienceDirect

Physica B

journal homepage: www.elsevier.com/locate/physb

A study of electric-field-induced second-harmonic generation in asymmetrical Gaussian potential quantum wells

Wangjian Zhai*

College of Physical Science and Technology, Yulin Normal University, Yulin 537000, PR China

ARTICLE INFO

Article history:
Received 21 June 2014
Received in revised form
11 July 2014
Accepted 16 July 2014
Available online 27 July 2014

Keywords:
Second-harmonic generation
Gaussian potential
Quantum wells
Electric field

ABSTRACT

Electric-field-induced second-harmonic generation in asymmetrical Gaussian potential quantum wells is investigated using the effective mass approximation employing the compact density matrix method and the iterative approach. Our results show that the absolute value, the real part and the imaginary part of second-harmonic generation are greatly affected by the height of the Gaussian potential quantum wells, the range of the Gaussian confinement potential and the applied electric field. The relationship between the absolute value and the imaginary part of second-harmonic generation together with the relationship between the absolute value and the real part of second-harmonic generation is studied. It is found that no matter how the height of the Gaussian potential quantum wells, the range of the Gaussian confinement potential and the applied electric field vary, the resonant peaks of the absolute value of second-harmonic generation do not originate from the imaginary part but from the real part.

1. Introduction

The characteristics of optical and electronic properties in nano-materials have been so intensively studied for many years because of their novel physical characteristics and applications in opto-and nanoelectronics. Many remarkable effects such as nonlinear optical effects [1–3], quantum plasmon effects [4,5] and giant magnetoresistance effects [6,7] in nano materials are investigated. The physical origin for those remarkable effects above in nano materials is that nano materials exhibit unique optical and electronic properties very different from their bulk counterparts, resulting from their enhanced quantum confinement effects. In recent years with the remarkable growth of nanotechnology, the synthesis of nano materials has strongly developed due to great advances that allow us to manipulate materials at the nanometer scale at an unprecedented level of precision. Thus, we can prepare for a diverse set of nano materials by controlling size, shape and chemical environment, and we can do research on optical and electronic properties in nano materials from experimental aspects. To fully understand and predict experimental phenomenon, theoretical studies are required that achieve a full description of nano materials. Nonlinear optical properties in nano materials such as quantum dots, quantum wells and quantum wire also have been so intensively studied theoretically [1–3,8–17]. The considerable attention for nonlinear optical properties is due to their potential applications in far-infrared laser amplifiers [18], far-infrared photodetectors [19], and high-speed, electro-opticalmodulators [20].

Nonlinear optical effects include odd-order and even-order ones. For nano materials of symmetric structure, even-order nonlinear optical effects are usually very small except for the contribution of the bulk susceptibility [21]. There are usually two ways to break the inversion symmetry of nano materials: using advanced material growing technology and applying an electric field [3]. In this paper, a theoretical model with asymmetrical confinement potential in the presence of electric field is employed to study second-harmonic generation (second-order nonlinear optical effects). Second-harmonic generation in asymmetrical structures or applying electric field such as semi-parabolic quantum wells [3], parabolic quantum dots with electric and magnetic fields [22], semi-exponential quantum wells [23], asymmetric coupled quantum wells [24], Pöschl–Teller quantum wells under the intense laser field [25], and semi-parabolic and semi-inverse squared quantum wells [26] was reported. From the work above, it is obvious that larger second-harmonic generation is obtained by changing electric field and adjusting structure parameters. In our paper, the confinement potential is asymmetrical Gaussian potential. The confinement potential is approximately the parabolic potential in GaAs/AlGaAs and InGaAs/GaAs/AlAs quantum dots [27–29]. However, experiment shows that the confinement potential is not approximately the parabolic potential but the Gaussian potential [30]. Based on the Gaussian potential, related work associated with nonlinear optical properties was reported. For example, Lu, Xie and Hassanbadi investigated nonlinear optical properties in quantum dots with Gaussian potential and donor

* Tel.: +86 18078506573.
E-mail address: zhaiwangjian@126.com

http://dx.doi.org/10.1016/j.physb.2014.07.030
0921-4526/

impurities under laser field [31]. Guo and Du studied linear and nonlinear optical absorption and refractive index changes in quantum wells with asymmetrical Gaussian potential and applied electric field [32]. Wu, Guo and Liu investigated polaron effects on nonlinear optical rectification in asymmetrical Gaussian potential quantum wells with applied electric fields [33]. Novel nonlinear optical effects are obtained in the work above. Therefore, it is necessary to give a detailed study of second-harmonic generation in asymmetrical Gaussian potential quantum wells with applied electric fields.

2. Model and theory

We consider an electron with charge e and effective mass m^* confined in asymmetrical Gaussian potential quantum wells whose form can be seen in Eq. (2). The external electric field F is applied in the z-direction. Within the framework of effective mass approximation, the Hamiltonian of the system can be written as

$$H = -\frac{\hbar^2\nabla^2}{2m^*} + V(z) + eFz, \tag{1}$$

with

$$V(z) = \begin{cases} -V_0 \exp(-z^2/2L^2) & z \geq 0 \\ \infty & z < 0, \end{cases} \tag{2}$$

Here, z represents the growth direction of the quantum wells. $\hbar$ is the Planck constant. V_0 is the barrier height of the Gaussian potential quantum wells and L is the range of the confinement potential. The parameters V_0 and L have great influences on asymmetrical Gaussian potential. The influences are exhibited in Fig. 1. The solutions of the Hamiltonian in Eq. (2) can be obtained by the methods used by the Refs. [32–34]. Bloch theory is used to deal with the Hamiltonian H_{xy} in the x–y plane. Therefore, the solutions of the Hamiltonian H can be obtained as

$$\psi_{n,\mathbf{k}}(\mathbf{r}) = \phi_n(z) u_c(\mathbf{r}) e^{i\mathbf{k}_\parallel \cdot \mathbf{r}_\parallel}, \tag{3}$$

and

$$\varepsilon_{n,\mathbf{k}} = E_{n,z} + \frac{\hbar^2 \mathbf{k}_\parallel^2}{2m^*}. \tag{4}$$

where $u_c(\mathbf{r})$ is the periodic part of the Bloch function in the conduction band at $\mathbf{k}=0$. $\phi_n(z)$. $E_{n,z}$ can be obtained by solving the following Schrödinger equation:

$$H_z\phi_n(z) = \left[-\frac{\hbar^2}{2m^*}\frac{\partial^2}{\partial z^2} + V(z) + eFz\right]\phi_n(z) = E_{n,z}\phi_n(z), \tag{5}$$

For $z/L \ll 1$, the Gaussian potential can be approximated by $-V_0(1-z^2/2L^2)$. Setting $\alpha = (m_e V_0)^{1/4}/(\hbar L)^{1/2}$, the solution of Eq. (5) can be obtained as

$$E_{n,z} = (2n+3/2)\sqrt{\frac{V_0\hbar^2}{m^*L^2}} - V_0 - \frac{e^2F^2L^2}{2V_0}, \quad n = 0, 1, 2\ldots, \tag{6}$$

and

$$\phi_n(z) = \sqrt{\frac{\alpha}{(2^n n!\sqrt{\pi})}} e^{-\alpha^2 z^2/2} H_n\left[\alpha\left(z - \frac{eFL^2}{V_0}\right)\right], \tag{7}$$

where $H_n(\alpha z)$ is Hermite polynomials.

Next, we will present a formalism for the derivation of second-harmonic generation coefficient by the compact density matrix method and the iterative procedure. Suppose our system is excited by an electromagnetic field. The electric field vector of the electromagnetic field is

$$E(t) = E_0 \cos(\omega t) = \tilde{E}\exp(-i\omega t) + \tilde{E}\exp(i\omega t), \tag{8}$$

where ω is the frequency of the external incident field. After neglecting the terms which contribute to our calculations, the electronic polarization of the system due to the internal field can be expressed as

$$P(t) = \varepsilon_0 \chi_{2\omega}^{(2)} \tilde{E}^2 e^{2i\omega t} + c.c, \tag{9}$$

where ε_0 is the vacuum permittivity, and $\chi_{2\omega}^{(2)}$ the second-harmonic generation (SHG). With the compact density matrix approach and the iterative procedure, the analytical expression for the second-harmonic generation is given as [3,22–26]

$$\chi_{2\omega}^{(2)} = \frac{e^3\sigma_v}{\varepsilon_0\hbar^2} \frac{M_{01}M_{12}M_{20}}{(\omega - \omega_{10} + i\Gamma_{10})(2\omega - \omega_{20} + i\Gamma_{20})}, \tag{10}$$

where $M_{01} = |\langle\psi_1|z|\psi_0\rangle|$, $M_{12} = |\langle\psi_2|z|\psi_1\rangle|$ and $M_{20} = |\langle\psi_2|z|\psi_0\rangle|$ are the off-diagonal matrix elements. $\hbar\omega_{10} = E_1 - E_0$, $\hbar\omega_{20} = E_2 - E_0$. σ_v is the electron density in the system. $\Gamma_{10} = \Gamma_{20} = \Gamma$. Γ is the phenomenological relaxation rate. The SHG susceptibility has a resonant peak in the energy position of two-photon resonance $\hbar\omega = \hbar\omega_{10} = \hbar\omega_{20}/2$, obtained by

$$\chi_{2\omega,max}^{(2)} = \frac{e^3\sigma_v}{\varepsilon_0} \frac{M_{01}M_{12}M_{20}}{(\hbar\Gamma)^2} \tag{11}$$

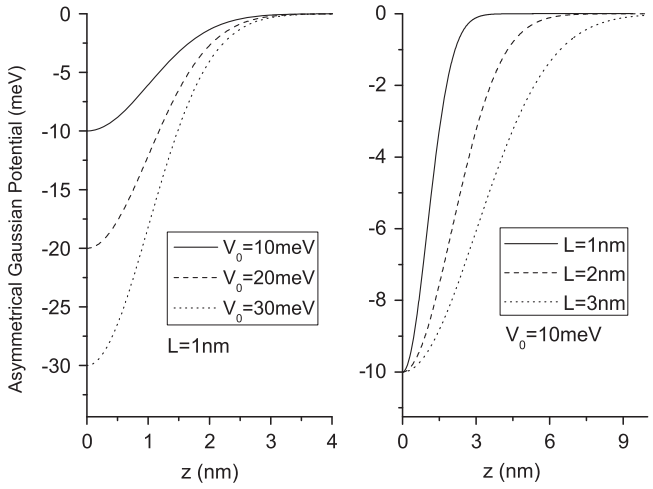

Fig. 1. The schematic representation of asymmetrical Gaussian potential.

3. Results and discussions

In this section, electric-field-induced second-harmonic generation (SHG) in asymmetrical Gaussian potential quantum wells is calculated numerically. The parameters adopted are as follows: $m^* = 0.067\, m_0$ (where m_0 is the electron mass), $\Gamma = 1/0.2\ ps$, $\varepsilon_0 = 8.85 \times 10^{-12}$ F m^{-1} and $\sigma_v = 5.0 \times 10^{24}$ m^{-3} [32,33].

Fig. 2 shows the SHG coefficients $|\chi_{2\omega}^{(2)}|$ as a function of the incident photon frequency ω, with $V_0 = 10$ meV, $F = 0$ kV/cm and $F = 100$ kV/cm for three different values of L. L is set as 1 nm, 1.5 nm and 2 nm, respectively. From Fig. 2, we can see that the magnitudes of $|\chi_{2\omega}^{(2)}|$ increase when applying electric field. For example, for $L = 2$ nm, the resonant peak of $|\chi_{2\omega}^{(2)}|$ with $F = 100$ kV/cm is over 90 times than that with $F = 0$ kV/cm. From the figure, it is clearly observed that with the increase of L, the resonant peaks of $|\chi_{2\omega}^{(2)}|$ shift to lower energy regions (red shift). The reason for the red shift is that with the increase of L, quantum confinement gets weakened. Therefore, the energy interval E_{ij} between difference quantum states decreases with increasing L. Besides, it is also seen that the magnitudes